Optics Letters

Iodine-stabilized single-frequency green InGaN diode laser

Yi-Hsi Chen,[1] Wei-Chen Lin,[1] Jow-Tsong Shy,[2] and Hsiang-Chen Chui[1,*]

[1]Department of Photonics, National Cheng-Kung University, Tainan 70101, Taiwan
[2]Department of Physics, National Tsing Hua University, Hsinchu 30013, Taiwan
*Corresponding author: hcchui@mail.ncku.edu.tw

Received 9 October 2017; revised 19 November 2017; accepted 30 November 2017; posted 1 December 2017 (Doc. ID 306892); published 22 December 2017

A 520-nm InGaN diode laser can emit a milliwatt-level, single-frequency laser beam when the applied current slightly exceeds the lasing threshold. The laser frequency was less sensitive to diode temperature and could be finely tuned by adjusting the applied current. Laser frequency was stabilized onto a hyperfine component in an iodine transition through the saturated absorption spectroscopy. The uncertainty of frequency stabilization was approximately 8×10^{-9} at a 10-s integration time. This compact laser system can replace the conventional green diode-pumped solid-state laser and applied as a frequency reference. A single longitudinal mode operational region with diode temperature, current, and output power was investigated. © 2017 Optical Society of America

OCIS codes: (140.2020) Diode lasers; (300.6260) Spectroscopy, diode lasers; (300.6460) Spectroscopy, saturation; (140.3425) Laser stabilization; (140.3570) Lasers, single-mode; (240.6680) Surface plasmons.

https://doi.org/10.1364/OL.43.000126

Single-frequency lasers have vital roles in the high-resolution spectroscopic analysis of atomic transitions and molecular hyperfine structures. Single-frequency lasers with watt-level output and sub- megahertz linewidths have been developed and commercialized. Laser diodes (LDs) are compact, low-cost laser sources with high effectiveness and low driving voltage. External feedback mechanisms are used to realize the single-frequency operation of LDs.

Single-frequency LDs are typically designed by selecting laser cavities with single-longitudinal modes (SLMs) and controlling mode parameters. The use of external cavity diode lasers (ECDLs) promises the development of a single-frequency laser within all potential frequencies. Wavelength-dispersive components with extended cavities can be used to select SLM and stabilize the laser frequency with the appropriate elements. An SLM is controlled using a piezoelectrically mounted mirror or grating. However, the advantages of LDs, such as compactness, stability, and simplicity of operation, are often lost when these techniques are applied. Moreover, mode hops occur when the LD frequency is tuned. Even if the operation temperature and current of the LDs are stabilized, the environmental conditions of the external cavity may affect the stability of the laser frequency.

Distributed Bragg reflector (DBR) LDs were developed in conjunction with advances in the semiconductor fabrication technique. The architecture of DBR LDs consists of a gain region and one or two separate DBR grating regions that are monolithically fabricated over a ridge waveguide. The DBR grating functions as a frequency-dependent mirror and is integrated near the gain medium. The distributed feedback (DFB) structure provides a compact single-frequency LD design. However, the DFB structure limits designed wavelength regions. Narrow-linewidth, single-frequency DFB LDs have been well developed, given their importance as light sources in optical communication bands [1]. In addition, techniques for single-frequency LDs in the near-infrared region are well established and several frequency references linked to alkali atomic transitions have been obtained.

The use of single-frequency lasers as frequency makers within the blue–green region relies on frequency doubling from near-infrared lasers. Single-frequency lasers have been achieved by doubling the frequency of diode-pumped 1064 nm Nd-doped solid-state lasers [2] or 976 nm diode lasers [3]. The emission of a high-power green laser from a 1060 nm DBR laser and a frequency doubler has been demonstrated [4]. Agnesi *et al.* [2] designed and characterized a diode-pumped, intracavity-doubled continuous-wave (cw) Nd:YAG laser with single-longitudinal and transverse modes and obtained >600 mW 532 nm output. Nevertheless, high-output power in a single frequency within the green region is still desired [5]. A cw single-frequency laser with dual wavelengths at 1064 and 532 nm has been recently reported [6]. The narrow-linewidth ECDLs at the blue region were reported [7,8].

Researchers have aimed to develop green LDs for miniaturized laser systems. Yanashima *et al.* [9] designed milliwatt-level green-visible indium gallium nitride (InGaN) LDs and then attempted to lower the threshold current of the LDs [9]. OSRAM Opto Semiconductors released a 120 mW 520 nm laser in 2014. The development of OSRAM green LDs is described in Ref. [10], and the measurement of their

electro-optical parameters is reported in Ref. [11]. Then we attempted to integrate this LD into an ECDL system, and at first examined the laser output spectrum with LD operation current. We found that the LD output spectrum showed a nearly SLM when the low applied current slightly exceeds the threshold. Then additional longitudinal modes developed with increasing LD current. We fine-tuned the LD temperature and current to obtain a 522 nm diode laser that can function as a single-frequency laser with low milliwatt output. This laser has potential applications in spectroscopic analysis. We investigated the operations of laser modes with applied current. We then identified the same optical characteristics—a single-frequency beam emitted by an InGaN green LD just above the lasing threshold—in other OSRAM green LDs (Thorlabs L520P120) purchased from Thorlabs.

In this Letter, we identified the operational region for a SLM between the lasing threshold (Ith) and 1.04 Ith. We also observed abrupt mode hopping (approximately 0.41 nm) with applied current. This mode has been previously designated as mode clustering and explained clearly by Weig *et al.* [12]. We then attempted to stabilize the laser frequency onto the differential signals of iodine hyperfine transitions. Frequency stabilization in tens of megahertz and operational time in tens of minutes were achieved. This compact scheme can replace conventional green diode-pumped solid-state lasers and be applied as frequency standards.

We measured the lasing spectrum of LDs under different LD temperatures and applied currents. The LD (OSRAM PLP520 B1) was mounted on a temperature-controlled aluminum plate and driven by a low-noise quantum-cascaded laser (QCL) driver (Wavelength Electronics QCL500) at 7 V operating voltage. The maximal output power increased to 100 mW under 340 mA, and the lasing threshold current was measured as 142 mA at 15°C. An ultrahigh resolution monochromator (Jobin Yvon iHR550, Horiba) was employed to scan the whole spectrum at different operational currents and temperatures. The monochromator was used with the following conditions: exit slit width of 2 μm, grating of 1800 line/mm, and integration time of 0.1 s. The resolution was set as 0.003 nm or approximately 3.3 GHz when the central wavelength was 522 nm. The green LD spectra for the operational currents at 140, 150, and 160 mA when the LD temperature was set as 15°C are shown in Fig. 1. Here the baselines of two spectral curves are shifted. The spectral baseline of 150 mA is shifted up to 30,000, and one of 160 mA is shifted up to 90,000. The spectrum of a 140 mA current appeared similar to that of a light-emitting diode. Spontaneous emissions dominate the spectrum when the LD operated under the lasing threshold. When the LD current increased to 142 mA, the linewidth narrowed to 5.1 GHz, and the LD lased with only a SLM inside. When the LD current was 146 mA, the mode linewidth was 3 GHz, which is lower than the resolution of the monochromator. We employed a Fabry–Perot interferometer (Thorlabs SB200-3B) to identify the actual linewidth of the green LD. We found that its actual linewidth was 41 MHz when the LD current was 146 mA. When the LD current was tuned to 160 mA, the spectrum exhibited a longitudinal mode spacing of 0.24 THz. Although the SLM occurred only at low operational current, the green LD can deliver a 10 mW laser under 150 mA current, which is sufficient for many spectroscopic studies. Figure 2 shows that the peak wavelength

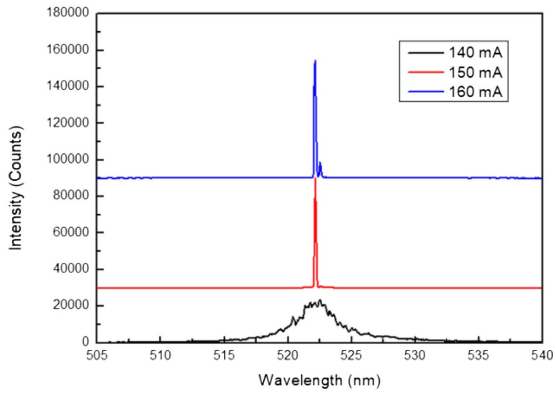

Fig. 1. Typical LD lasing spectra of currents applied at 140, 150, and 160 mA. The LD temperature is 15°C. The baseline of spectral 150 mA is shifted up to 30,000, and one of 160 mA is shifted up to 90,000.

was achieved by varying the applied current from under the lasing threshold to 150 mA. The peak wavelength remained constant within the region of the applied current in which mode hopping was found.

Wavelength tuning with the LD temperature was 38.1 pm/K and was less sensitive to temperature variations. This phenomenon was originally discovered by Eichler *et al.* [13] in InGaN-based LDs. Avramescu *et al.* [10] obtained a wavelength tuning value with the LD temperature of 0.04 nm/K. This optical characteristic reduced the effort required to maintain a high precision temperature of green LDs. By first selecting the peak wavelength to avoid mode hopping with the applied current, we found that the peak wavelength tuning with the applied current was 2.8 pm/mA (137–146 mA) and 3.1 pm/mA (146–150 mA). Thus, we obtained SLM operation, albeit in a narrow current window.

The experimental setup is shown in Fig. 3. The LD was mounted on a temperature-controlled aluminum plate and driven by a QCL driver. A plano-convex lens with 15 mm focal length was placed on the laser exit and used as a beam collimator. The vertical linear polarization direction was converted to the circular polarization direction by a quarter-wave plate (QWP) before the laser beam was sent to an iodine cell.

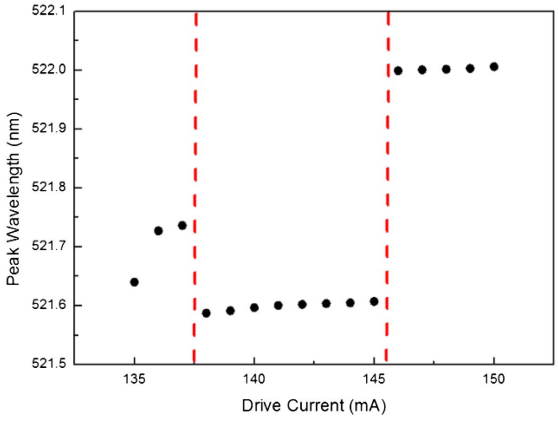

Fig. 2. Location of peak wavelength as a function of operational current. The LD temperature is 15°C.

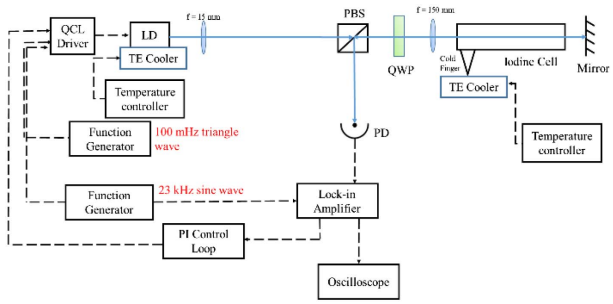

Fig. 3. Experimental scheme for an iodine-stabilized LD. PBS, polarizing beam splitter; PD, photodetector; QWP, quarter-wave plate; PI, proportional-integral; REF, reference.

A mirror reflected the transmitted beam, and near-perfect alignment can be achieved adjusting the mirror. The signal from the photodetector (Thorlabs PDA100) was demodulated with a lock-in amplifier (Stanford Research System SR830). The current of the laser was modulated at fmod = 30 kHz with a 30 MHz modulation depth. The iodine cell was 50 mm in length and maintained at room temperature. The cold finger of the iodine cell was placed in ice water and maintained near ice point to control vapor pressure.

Frequency-stabilized lasers are essential as frequency references or local oscillators in numerous applications, including high-resolution molecular and atomic spectroscopy [14], and in precision measurement and laser cooling experiments. The laser frequency is locked to specific atomic or molecular transitions [15] or comb lines from an optical frequency comb [16]. Here we used iodine saturation spectroscopy [17] to reveal the hyperfine structure of iodine in the 520 nm region. Moreover, we locked the laser frequency to a sub-Doppler linewidth. Information on iodine transitions, including transition frequencies, intensities, and hyperfine structure, can be cross-referenced to atlases written by Gerstenkorn and Luc [18]. Furthermore, iodine frequencies higher than 2 MHz over an extensive frequency range can be predicted using IodineSpec 5, a program from Knockel and Tiemann on the basis of the model descriptions of hyperfine [19] and rovibronic [20,21] structures. Cheng *et al.* [22] explored sub-Doppler transitions of iodine molecules in the blue–green region (wavelength range 523–498 nm) using a frequency-doubled Ti:sapphire laser.

A Doppler-broadened iodine spectrum was obtained through one-way absorption with amplitude modulation using an acousto-optic modulator. The transition was identified as the P(45) 38-0 transition. Its Doppler linewidth was 0.9 GHz, and its linear absorption contrast, the absorption intensity of the Doppler absorption signal compared with background, was 3×10^{-3}. The central frequency, 574267.1 GHz, of this transition was obtained using a wavemeter with 60 MHz accuracy (Bristol Instruments 671) and was in good agreement with the value of 574267.08 GHz given in IodineSpec 5.

Doppler-free saturation spectroscopy was then used to resolve the hyperfine components of the rovibronic transitions of the iodine molecule. The amplitude of the laser was modulated at 23 kHz. The signal from the photodetector was demodulated with a lock-in amplifier at the first-derivative frequency. The spectrum of the demodulated signal at the first derivative of the modulation frequency is shown in Fig. 4, in which the sub-Doppler hyperfine spectrum can easily be identified. The scan rate was 0.1 GHz/s, and the whole scan range was 1.2 GHz. The hyperfine transitions shown in Fig. 4 were identified as the a1–a21 components of the P(45) 38-0 transition. The signal-to-noise ratio was approximately 63 at the time constant of 300 ms. The first-derivative demodulated signal was a zero-crossing signal used to lock the laser frequency on the centers of iodine saturation–absorption lines. The highest signal was a combination of a5 and a6 components. Although individual hyperfine components were not completely resolved because of pressure broadening and laser linewidths, the zero-crossing signal could still be used to stabilize the laser frequency to a tens of megahertz level. We selected component a4 to provide the locking signal to modulate the laser frequency given that no peaks near the a4 component in the lower frequency side and a5 + a6 components were easily identified. The demodulated signal was fed to the proportional-integral control loop to control the LD operational current. The time trace of the error signal when the laser was locked is shown in Fig. 5. The locking signal was shown in the inset figure. The time constant of the lock-in amplifier was

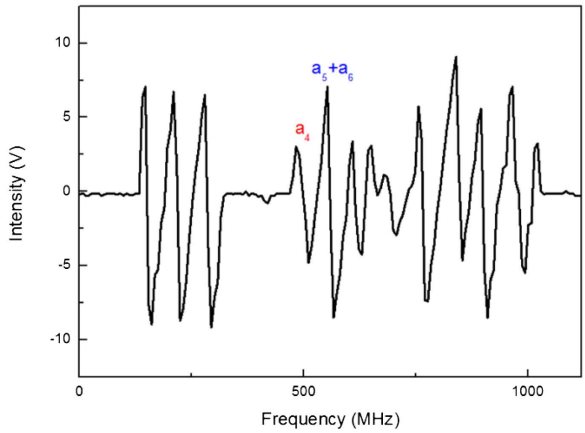

Fig. 4. First-derivative demodulated saturated–absorption spectrum. The hyperfine structure of iodine was identified as a1–a15 components of the P(45) 38-0 transition. The signal-to-noise ratio is 63 at the time constant of 300 ms.

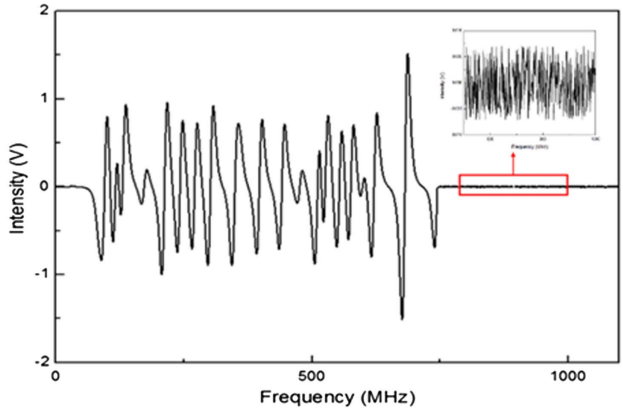

Fig. 5. Typical trace of the first-derivative demodulated signal of the laser locked to the a4 component. Inset: the locking signals.

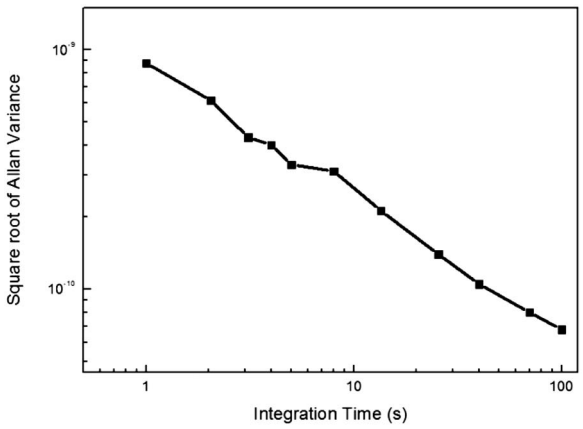

Fig. 6. Square root of Allan variance as a function of measurement time.

300 ms. The peak-to-peak frequency jitter was estimated from the locked error signal to be 31 MHz at 522 nm.

We also used a series of measurements taken at different measurement times to calculate the square root of the Allan variance, as shown in Fig. 6. The frequency instability estimated from the locked error signal was 8×10^{-9} (10 s), which corresponded to a frequency variation of 4.4 MHz at 522 nm. This value is approximately one-tenth of the LD linewidth.

To the best of our knowledge, we are the first to observe the saturation–absorption spectrum of iodine by using a direct green InGaN LD. Although the LD was operated at low applied current, the efficient laser power resulted in good signal-to-noise ratio and permitted the direct locking of the laser frequency to the saturation–absorption line of the hyperfine structural transition of iodine. We obtained frequency stabilizations that are lower than other iodine frequency references. However, the green LDs exhibited temperature insensitivity and lacked mode hopping within a narrow current window. Given these features, green LDs are excellent candidates for frequency markers. The compact experimental scheme eliminates the need for an enhancement cavity or dispersive elements, such as a volume-grating mirror or grating. Therefore, secondary frequency references for the visible region can be obtained using an iodine-stabilized diode laser. This scheme can provide a feasible, compact frequency reference system for frequency standards within the green region. Higher frequency stabilization can be realized by higher laser power and narrower linewidth. Green ECDL can be a good candidate.

Funding. Ministry of Science and Technology, Taiwan (MOST) (104-2112-M-006-006-MY2, 104-2738-M-006-003).

Acknowledgment. The authors thank Prof. Chin-Chun Tsai for the use of the equipment.

REFERENCES

1. H. C. Chui, M. S. Ko, Y. W. Liu, T. Lin, J. T. Shy, S. Y. Shaw, R. V. Roussev, and M. M. Fejer, Opt. Lasers Eng. **44**, 479 (2006).
2. A. Agnesi, S. DellAcqua, G. C. Reali, P. G. Gobbi, and D. Ragazzi, Appl. Opt. **36**, 597 (1997).
3. A. Jechow, M. Schedel, S. Stry, J. Sacher, and R. Menzel, Opt. Lett. **32**, 3035 (2007).
4. M. H. Hu, N. Hong Ky, S. Kechang, L. Yabo, N. J. Visovsky, L. Xingsheng, N. Nishiyama, S. Coleman, L. C. Hughes, J. Gollier, W. Miller, R. Bhat, and Z. Chung-En, IEEE Photon. Technol. Lett. **18**, 616 (2006).
5. H. D. Lu, J. Su, Y. H. Zheng, and K. C. Peng, Opt. Lett. **39**, 1117 (2014).
6. C. W. Zhang, H. D. Lu, Q. W. Yin, and J. Su, Appl. Opt. **53**, 6371 (2014).
7. B. Li, J. Gao, A. L. Yu, S. W. Luo, D. S. Xiong, X. B. Wang, and D. L. Zuo, Opt. Laser Technol. **96**, 176 (2017).
8. D. Ding, X. Q. Lv, X. Y. Chen, F. Wang, J. Y. Zhang, and K. J. Che, Opt. Laser Technol. **94**, 1 (2017).
9. K. Yanashima, H. Nakajima, K. Tasai, K. Naganuma, N. Fuutagawa, Y. Takiguchi, T. Hamaguchi, M. Ikeda, Y. Enya, S. Takagi, M. Adachi, T. Kyono, Y. Yoshizumi, T. Sumitomo, Y. Yamanaka, T. Kumano, S. Tokuyama, K. Sumiyoshi, N. Saga, M. Ueno, K. Katayama, T. Ikegami, and T. Nakamura, Appl. Phys. Express **5**, 082103 (2012).
10. A. Avramescu, T. Lermer, J. Muller, S. Tautz, D. Queren, S. Lutgen, and U. Strauss, Appl. Phys. Lett. **95**, 071103 (2009).
11. T. Hager, G. Bruderl, T. Lermer, S. Tautz, A. Gomez-Iglesias, J. Muller, A. Avramescu, C. Eichler, S. Gerhard, and U. Strauss, Appl. Phys. Lett. **101**, 171109 (2012).
12. T. Weig, T. Hager, G. Bruderl, U. Strauss, and U. T. Schwarz, Opt. Express **22**, 27489 (2014).
13. C. Eichler, S. S. Schad, F. Scholz, D. Hofstetter, S. Miller, A. Weimar, A. Lell, and V. Harle, IEEE Photon. Technol. Lett. **17**, 1782 (2005).
14. H. C. Chui, Y. W. Liu, J. T. Shy, S. Y. Shaw, R. V. Roussev, and M. M. Fejer, Appl. Opt. **43**, 6348 (2004).
15. C. M. Wu, T. W. Liu, M. H. Wu, R. K. Lee, and W. Y. Cheng, Opt. Lett. **38**, 3186 (2013).
16. T. W. Liu, C. M. Wu, Y. C. Hsu, and W. Y. Cheng, Appl. Phys. B **117**, 699 (2014).
17. H.-C. Chui, S.-Y. Shaw, M.-S. Ko, Y.-W. Liu, J.-T. Shy, T. Lin, W.-Y. Cheng, R. V. Roussev, and M. M. Fejer, Opt. Lett. **30**, 646 (2005).
18. S. Gerstenkorn and P. Luc, *Atlas Du Spectre D'Absorption De La Molécule D'Iode, 14800–20000 cm^{-1}* (Centre national de la recherche scientifique, 1978).
19. E. J. Salumbides, K. S. E. Eikema, W. Ubachs, U. Hollenstein, H. Knoeckel, and E. Tiemann, Mol. Phys. **104**, 2641 (2006).
20. H. Knockel, B. Bodermann, and E. Tiemann, Eur. Phys. J. D **28**, 199 (2004).
21. E. J. Salumbides, K. S. E. Eikema, W. Ubachs, U. Hollenstein, H. Knockel, and E. Tiemann, Eur. Phys. J. D **47**, 171 (2008).
22. W. Y. Cheng, L. S. Chen, T. H. Yoon, J. L. Hall, and J. Ye, Opt. Lett. **27**, 571 (2002).